Cancer Control
Volume 31: 1–11

DOI: 10.1177/10732748241238616
journals.sagepub.com/home/ccx

CCL21 and CLDN11 Are Key Driving Factors of Lymph Node Metastasis in Gastric Cancer

Shaofei Yang, MMed[1,*], Dandan Dong, MMed[1,*], Xunxia Bao, MS[2], Rongting Lu, BS[3], Pufei Cheng, BS[4], Sibo Zhu, MD[5], and Guanghua Yang, MMed[1]

Abstract

Background: Gastric cancer (GC) is a leading cause of cancer-related deaths worldwide. Understanding the molecular mechanisms of GC metastasis is crucial for improving patient survival outcomes.

Methods: RNA sequencing and analysis were performed on tissue samples from primary and lymph node metastatic lesions of gastric cancer. Differential gene analysis and functional pathway analysis were conducted. Immune infiltrating environment and protein expression levels were evaluated using immunohistochemistry. Cell experiments were conducted to investigate the role of CCL21 in GC metastasis.

Results: ACTG2, CNN1, DES, MUC6, and PGC were significantly upregulated in primary tumor cells, while CCL21, MS4A1, CR2, CLDN11, and FDCSP were significantly upregulated in metastatic tumor cells. Functional pathway analysis revealed enrichment in pathways related to immune response. CLDN11 and CCL21 were found to play important roles in promoting gastric cancer metastasis. Cell experiments confirmed the role of CCL21 in promoting GC cell growth and metastasis. CCL21 is highly expressed in GC tissues and binds to CCR7, leading to upregulation of CLDN11. This results in GC-lymph node metastasis and abnormal activation of immune cells (B cells and $CD4^+$ T cells).

Conclusion: Inhibition of CCL21 and CLDN11 proteins may be a promising strategy for treating GC and preventing lymph node metastasis. These findings provide specific molecular markers for early lymph node metastases of GC, which can aid in developing treatment strategies and predicting patient prognosis.

Keywords

gastric cancer, metastasis, CCL21, CLDN11, biomarker

Received June 30, 2023. Received revised February 10, 2024. Accepted for publication February 22, 2024.

Introduction

Gastric cancer (GC) is a common malignancy worldwide with poor prognosis, posing a serious threat to human health. According to statistics from the International Agency for Research on Cancer, in 2012, there were approximately 951,000 new cases of GC and 723,000 deaths due to GC, ranking fifth in the incidence rate and third in the mortality rate of malignant tumors. More than 70% of new cases of GC occur in developing countries, with about 50% of cases occurring in East Asia, mainly concentrated in China. The number of cases and deaths due to GC in China accounts for

[1]Department of General Surgery, Seventh People's Hospital, Shanghai University of Traditional Chinese Medicine, Shanghai, China
[2]School of Life Science, Anhui Medical University, Hefei, China
[3]Shanghai Starriver Bilingual School, Shanghai, China
[4]Dipont-Huayao Collegiate School Kunshan, Suzhou, China
[5]School of Life Sciences, Fudan University, Shanghai, China

*Shaofei Yang and Dandan Dong contributed equally to this work.

Corresponding Authors:
Sibo Zhu, School of Life Sciences, Fudan University, 2005 Songhu Road, Shanghai 200438, China.
Email: sibozhu@fudan.edu.cn

Guanghua Yang, Department of General Surgery, Seventh People's Hospital, Shanghai University of Traditional Chinese Medicine, No. 358, Datong Road, Pudong New Area, Shanghai 200137, China.
Email: yangguanghualove@163.com

42.6% and 45.0%, respectively, of the total global number, ranking fifth in incidence rate and sixth in mortality rate among 183 countries worldwide.[1]

GC is a multifactorial disease with many factors affecting its development, including environmental and genetic factors. As a highly invasive and heterogeneous malignancy, GC remains a global health problem.[2] Studies have found that factors such as family history, diet, alcohol consumption, smoking, *Helicobacter pylori* infection, and Epstein-Barr virus infection significantly increase the risk of developing GC. Research has shown that deaths caused by the primary tumor account for only 10% of deaths caused by the tumor, with the majority of patients dying from distant metastasis.[3] In GC, lymph node metastasis has long been recognized as an important factor affecting patient prognosis.[4] At the population level, two primary prevention activities for GC may include improving dietary habits and reducing the incidence of *H pylori* infection, which is the main cause of GC. Secondary prevention strategies involve utilizing existing resources, mainly endoscopic methods, as the gold standard for early detection.[5]

The occurrence and development of GC involve multiple molecular mechanisms, and studying them can help develop new treatment methods and prevention strategies. For example, carbohydrate antigen 19-9 (CA 19-9) is the most commonly used serum tumor marker for diagnosis or therapeutic monitoring of pancreatic cancer. In cases of GC, serum CA 19-9, carcinoembryonic antigen (CEA), carbohydrate antigen 72-4 (CA 72-4), and carbohydrate antigen 15-3 (CA 15-3) are important indicators for early diagnosis and therapeutic monitoring.[6,7]

In this study, RNA sequencing and analysis were performed on paraffin-embedded tissue samples from primary and lymph node metastatic lesions of GC. After comparing gene expression levels, it was found that ACTG2, CNN1, DES, MUC6, and PGC were significantly upregulated in primary tumor cells, while CCL21, MS4A1, CR2, CLDN11, and FDCSP were significantly upregulated in metastatic tumor cells. The expression level of CCL21 was significantly associated with the presence of T cell $CD4^+$ and B cell. Cell experiments confirmed the key role of CCL21-mediated CLDN11 in promoting GC metastasis. This study provides specific molecular markers for tumor cells in early lymph node metastases of GC, which may help in developing treatment strategies and predicting patient prognosis for GC lymph node metastasis.

Materials and Methods

Collection of Clinical Specimens

All patients participating in this study underwent pathological assessmentat the Seventh People's Hospital of Shanghai and received standard GC surgical resection. The study was approved by the Ethics Committee of the Seventh People's Hospital of Shanghai, approval number is 028 (2020). All patients included in this study signed informed consent forms. Patients' GC primary lesion (n = 10) and lymph node metastasis paraffin tissue (n = 11) samples were included in this study.

RNA-Seq

RNA was extracted from the paraffin tissue samples using Qiagen RNeasy FFPE Kit (Qiagen, 73504). In order to extract sufficient RNA, 5 slices of 10 μm paraffin sections were used for each sample. Reverse transcription of RNA samples was used to prepare cDNA using the SmartScribe™ Reverse Transcriptase kit (Takara Bio Inc.). VANTS DNA Clean Beads (Vazyme Biotech, Co., Ltd.) was used to sort cDNA products, and TruePrep DNA Library Prep Kit V2 for Illumina (Vazyme Biotech, Co., Ltd.) was used to obtain 200- to 1000-bp fragments for preparing the cDNA library. All libraries were quantified using a 2100 Bioanalyzer and pooled at 1:1 at 2 nM for HiSeq 150 bp paired-end sequencing (Illumina, Inc.).

RNA-Seq Data Analysis

Use Trimmomatic software to preprocess the raw sequencing data, eliminating sequencing adapters and low-quality reads to ensure data quality and accuracy. Then, employ the HiSat2 tool to align the sequencing data with the human genome UCSC hg38 (https://genome-ftp.cse.ucsc.edu/goldenPath/hg38/chromosomes/) for accurate mapping of the sequencing sequences to the reference genome. Next, perform quantitative analysis of gene expression for each gene using the featureCounts software. Normalize the read counts to transcripts per million (TPM) values, and transform the TPM values to log2 scale using the "newSCESeSet" function in the R-project (version 3.5.2, https://www.r-project.org/) package "scater" to meet subsequent data analysis requirements. Finally, generate visual results such as heatmaps and dimensionality reduction plots based on the transformed data using the ggplot2 tool.

Differentially Expressed Genes (DEGs)

Utilize the edgeR model to perform differential gene expression analysis between the "treatment" and control groups, calculating statistical significance and fold change for each gene. Then, use the R package "ggplot2" to plot volcano plots and heatmaps for the Top 20 differentially expressed genes. The criteria for identifying Differentially Expressed Genes (DEGs) are $|\text{Log2 fold-change}| \geq 1$, $P < .05$. Subsequently, conduct KEGG pathway analysis and Gene Ontology (GO) analysis on the differentially expressed genes using the R package "clusterProfiler" to aid in understanding the functions of genes or proteins in biological organisms and the biological pathways they are involved in.

Gene Co-Expression Networks (Co-Network)

Utilize the AnimalTFDB (v3.0) database to select the top 20 differentially expressed genes that are transcription factors. Then, calculate the correlation coefficients between these transcription factors and other differentially expressed genes using the Pearson index. Finally, create a co-expression network diagram between the transcription factors and these differentially expressed genes using CytoScape (v3.4).

Estimating the Proportion of Immune and Cancer cells

EPIC incorporates non-negativity constraints into deconvolution problems using constrained least squares regression, estimating the proportions of immune and cancer cells from a large amount of tumor gene expression data. The total sum of cell fractions in each sample does not exceed one. The analysis is performed using the "EPIC" function in R package "immunedeconv."

Immunohistochemistry (IHC)

Samples were fixed in 10% Neutral Formalin Fix Solution (BBI Solutions), embedded in paraffin, and cut into 4-μm thick tissue sections. For antigen retrieval, tissue sections were placed in antigen retrieval buffer (pH 9.0; Wuhan Servicebio Technology, Co., Ltd.) for antigen retrieval in a microwave oven on medium power for 8 min until boiling, then cooled for 8 min and then switched to medium-low power for 7 min. After natural cooling, the slides were placed in PBS (pH 7.4; Wuhan Servicebio Technology, Co., Ltd.) and washed 3 times on a destaining shaker. Next, 3% hydrogen peroxide solution was incubated with the sample at room temperature for 25 min to block endogenous peroxidase, followed by blocking with 3% BSA (Sangon Biotech, Co., Ltd.) at room temperature for 30 min. The tissue sections were incubated with anti-ISG15 antibody (dilution, 1:100; cat. no. DF6316; Affinity Biosciences) at room temperature (RT) for 1 h. The HRP-labelled goat-anti-rabbit (dilution, 1:200; cat. no. G1213; Wuhan Servicebio Technology, Co., Ltd.) antibody was used for incubation at RT for 1 h. After the 3,3′-diaminobenzidine application for 5-10 min, the staining was observed under a microscope (CKX53; Olympus).

Western-Blot

Equal amounts of protein were loaded onto SDS-PAGE gels and separated by electrophoresis. The proteins were then transferred onto PVDF membranes and blocked with 5% non-fat milk. Membranes were incubated overnight at 4°C with primary antibodies (CCR7: abcam, ab191575; CLDN11: CST, 38062S, β-actin: CST, 4967S) specific to the target protein and subsequently incubated with secondary antibodies. Protein bands were visualized using an enhanced chemiluminescence system, and analysis was performed using ImageJ software.

Cell Counting Kit-8 Assay

The proliferation of cells in each group was detected using CCK-8 (Dojindo, Japan). Human GC cell lines HGC-27 and MKN28 (obtained from Cinoasia Institute) in logarithmic growth phase were seeded in 96-well plates at a density of 1×10^4 cells/well and incubated overnight at 37°C with 5% CO_2 in a cell culture incubator. Recombinant CCL21 protein was added to the experimental group, and 10 μL of CCK-8 (Dojindo, Japan) reagent was added to each well at zero h, 24 h, 48 h, and 72 h. After incubation at 37°C for 2 h, the OD values of each group were measured using an enzyme-linked immunosorbent assay reader (Thermo, USA) at a wavelength of 450 nm.

Cell Apoptosis Assay

HGC-27 and MKN28 cells were seeded in 6-well plates at a density of 1×10^5 cells/well and incubated overnight at 37°C with 5% CO_2 in a cell culture incubator. Recombinant CCL21 protein was added to the experimental group and incubated for 48 h. The cells were then collected by digestion and incubated with 5 μL Annexin V/FITC and 5 μL propidium iodide (PI) solution at room temperature for 30 min. The apoptotic rate of each group of cells was detected using a flow cytometer (BD Biosciences, USA).

Wound-Healing Assay

HGC-27 and MKN28 cells were seeded in 24-well plates at a density of 1×10^5 cells/well and incubated overnight at 37°C. When the cells reached over 90% confluence, a 10 μL pipette tip was used to scratch a straight line across the cell layer and marked. Recombinant CCL21 protein was added to the experimental group for intervention. The marked scratch area was photographed using an inverted microscope (Olympus, Japan) at 0 h and 24 h to observe the healing of the scratch. The scratch healing rate was calculated using Image J.

Transwell Assay

The logarithmic phase HGC-27 and MKN28 cells were suspended in 200 μL of serum-free RPMI1640 medium and seeded in the upper chamber of a Transwell plate (5×10^4 cells/well). Recombinant CCL21 protein was added to the experimental group, while 500 μL of complete medium (RPMI1640 and 10% fetal bovine serum) was added to the lower chamber. The cells were then incubated at 37°C with 5% CO_2 for 48 h. The cells in the upper chamber were removed with a cotton swab, fixed with 4% paraformaldehyde, stained with .5% crystal violet, and counted under

a microscope to determine the number of cells that had migrated through the membrane.

Statistical Analysis

Data were presented as the mean ± standard deviation (SD). Data were statistically analyzed using Prim 9. Statistical significance was determined by paired or non-paired Student's t test. $P < .05$ was considered statistically significant.

Results

Differential Gene Analysis Between Primary and Metastatic Lesions

Filtering was performed on the sequencing data: the expression matrix only retained protein-coding genes that were expressed in at least in 5 samples and had a summed expression level of at least 10 across all samples. After filtering, only 11857 genes remained. TPM normalization was then applied with log2 transformation to calculate Pearson correlation between samples, and carry out principal component analysis (PCA) (Figure 1(A)) and hierarchical clustering analysis (HCA) (Figure 1(B)), indicating relatively good distinction between sample groups. Using the edgeR package, differential gene expression (DEG) was analyzed on primary and metastatic tumor cells, discovering 1613 upregulated genes (higher expression in metastatic group than in primary group) and 352 downregulated genes (lower expression in metastatic group than in primary group). The top 20 differential expressed genes were selected and presented in a heatmap (Figure 1(C) and (D)). In the primary group cells, ACTG2, CNN1, DES, MUC6, and PGC were significantly upregulated, in the metastatic group cells, CCL21, MS4A1, CR2, CCR7, and FDCSP were significantly upregulated.

Functional Pathway Analysis

To analyze the role of differentially expressed genes between primary and metastatic lesions in GC metastasis, we used ClusterProfiler to perform enrichGOBP functional enrichment analysis on the 40 genes with the largest fold change. The results showed that these differentially expressed genes were enriched in immune response-regulating signaling pathways, B cell activation, T cell costimulation, and other functional pathways (Figure 2(A) and (B)). To explore the associated mechanisms of these differentially expressed genes in GC metastasis, we further screened for nuclear transcription factors among the differentially expressed genes and performed Spearman correlation analysis between the transcription factors and differentially expressed mRNAs. A TF-mRNA co-expression network diagram was generated, which showed that genes such as CLDN11, CCL21, and CCR7 play an important role in promoting GC metastasis (Figure 2(C)). Considering that CLDN11 and CCL21 may play a particularly important role in GC metastasis, we performed enrichGOBP functional enrichment analysis on the differentially expressed genes associated with them. The results showed that these differentially expressed genes were mainly enriched in immune response-regulating signaling pathways, B cell activation, regulation of humoral immune response, and other functional pathways (Figure 2(D)).

Immune Infiltration

To explore the immune infiltrating environment of primary and metastatic lesions, we used the immunedeconv R package to evaluate tumor immune infiltration for all samples. The analysis was performed using a unified method of estimating immune cell components from large-scale RNA sequencing data. From the results, we can clearly see that the proportion of B cells and $CD4^+$ T cells significantly increased in the metastatic lesions (Figure 3(A) and (B)). To investigate the potential correlation between immune cells in tumor tissue and CCL21 proteins, we calculated and analyzed the correlation between the expression levels of CCL21 and the relative abundance of immune cells. The results showed that the expression level of CCL21 was significantly associated with T cell $CD4^+$ and B cells (Figure 3(C)). In addition, the IHC results showed that lymphocytes secreted a large amount of CCL21 in the metastatic lesion tissue, while the tumor tissue secreted a large amount of CLDN11. Moreover, the expression levels of CCL21 and CLDN11 were significantly higher in the metastatic lesion tissue than in the primary lesion tissue (Figure 3(D)), indicating that CCL21 and CLDN11 play an important role in GC tumor immune infiltration and metastasis. Next, we downloaded RNA-seq data for Lymphoid Normal (LN) samples from the Genomic Data Commons (GDC) database (https://portal.gdc.cancer.gov/files/c88ad5e8-1430-41b3-b222-79af1a4da0c2). We compared the LN data with our Lymph Node Metastasis (MTT) samples and performed data normalization and differential analysis using the "limma" package in R. Genes with a P-value less than .05 and an absolute log fold change (logFC) greater than or equal to 1 were defined as differentially expressed genes. The volcano plot in Figure 3(E) shows the differential expression of genes, where CCL21 and CLDN11 were significantly upregulated in lymph node metastasis compared to normal lymphoid tissue, while CCR7 did not show significant differences. Figure 3(F) visualizes the differential expression levels of the three genes using box plots.

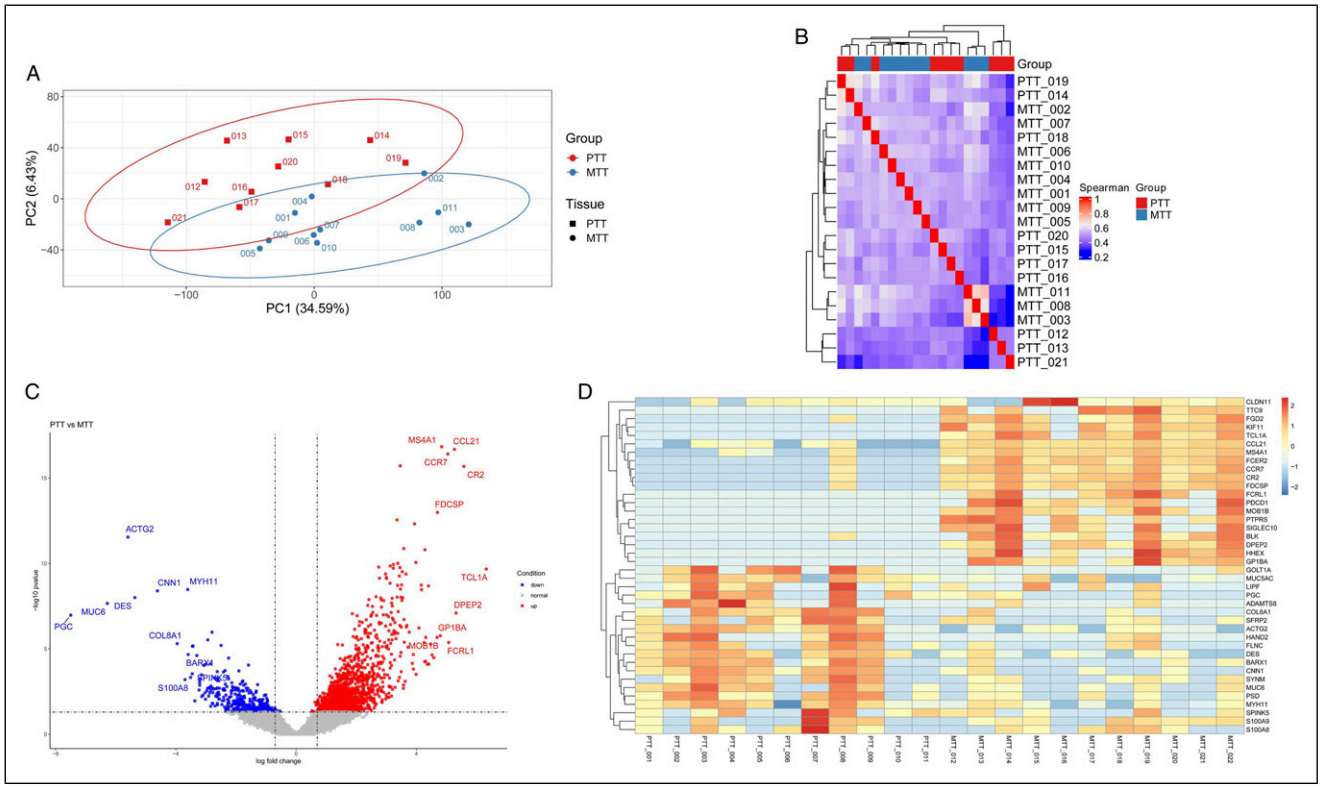

Figure 1. Differential gene analysis between primary and metastatic lesions. (A) Principal component analysis (PCA) plot showing the distinction between sample groups. (B) Hierarchical clustering analysis (HCA) dendrogram indicating relatively good separation of sample groups. (C) Volcano plot of the differentially expressed genes in metastatic and primary tumor. (D) Heatmap of the top 20 differentially expressed genes in metastatic and primary tumor.

CCL21 Promotes GC Cell Growth and Metastasis in Vitro

The mechanism of CCL21 in GC is still unclear. Based on the results of bioinformatics analysis, we speculate that CCL21 may be an important regulatory factor in the progression of GC metastasis. To investigate the functional role of CCL21 in GC cells, we treated human GC cell lines (HGC-27 and MKN28) with recombinant CCL21 protein and measured changes in the expression of CCR7 and CLDN11 genes as well as changes in cell proliferation, apoptosis, migration, and invasion abilities. qPCR and western-blot results showed that the expression levels of CCR7 and CLDN11 genes were significantly upregulated in GC-CCL21 cells (HGC-27 $P < .01$; MKN28 $P < .01$) (Figure 4(A) and(B)). CCK-8 assay results showed that CCL21 significantly promoted the proliferation of HGC-27 and MKN28 cells (HGC-27 $P < .05$; MKN28 $P < .05$) (Figure 4(C)). AnnexinV-PI flow cytometry detected no significant effect of CCL2 on apoptosis of the two GC cell lines (Figure 4(D) and (E)). Scratch test results showed that CCL2 significantly enhanced the migration ability of the 2 GC cell lines (HGC-27 $P < .001$; MKN28 $P < .01$) (Figure 5(A) and (B)). Transwell assay results showed that CCL21 significantly promoted the invasion ability of HGC-27 and MKN28 cells (HGC-27 $P < .01$; MKN28 $P < .05$) (Figure 5(C) and (D)).

Discussion

GC is the third leading cause of cancer-related deaths worldwide and the most common malignant tumor of the gastrointestinal tract in China. Although significant progress has been made in surgery and adjuvant therapy, the 5-year survival rate of GC patients remains low due to cancer recurrence caused by metastasis.[8] Therefore, elucidating the molecular mechanisms of GC metastasis is crucial for improving patient survival outcomes.

In this study, differential gene analysis was performed on the primary and metastatic lesions of GC. A total of 352 upregulated genes and 1613 downregulated genes were identified, and the top 20 differentially expressed genes were used to create a heatmap. The results showed that ACTG2, CNN1, DES, MUC6, and PGC were significantly upregulated in the primary group cells, while CCCL21, MS4A1, CR2, CLDN11, and FDCSP were significantly upregulated in the metastatic group cells. To further investigate the function of these differentially expressed genes, functional pathway analysis was performed and revealed that these genes were enriched in pathways such as lymphocyte activation involved

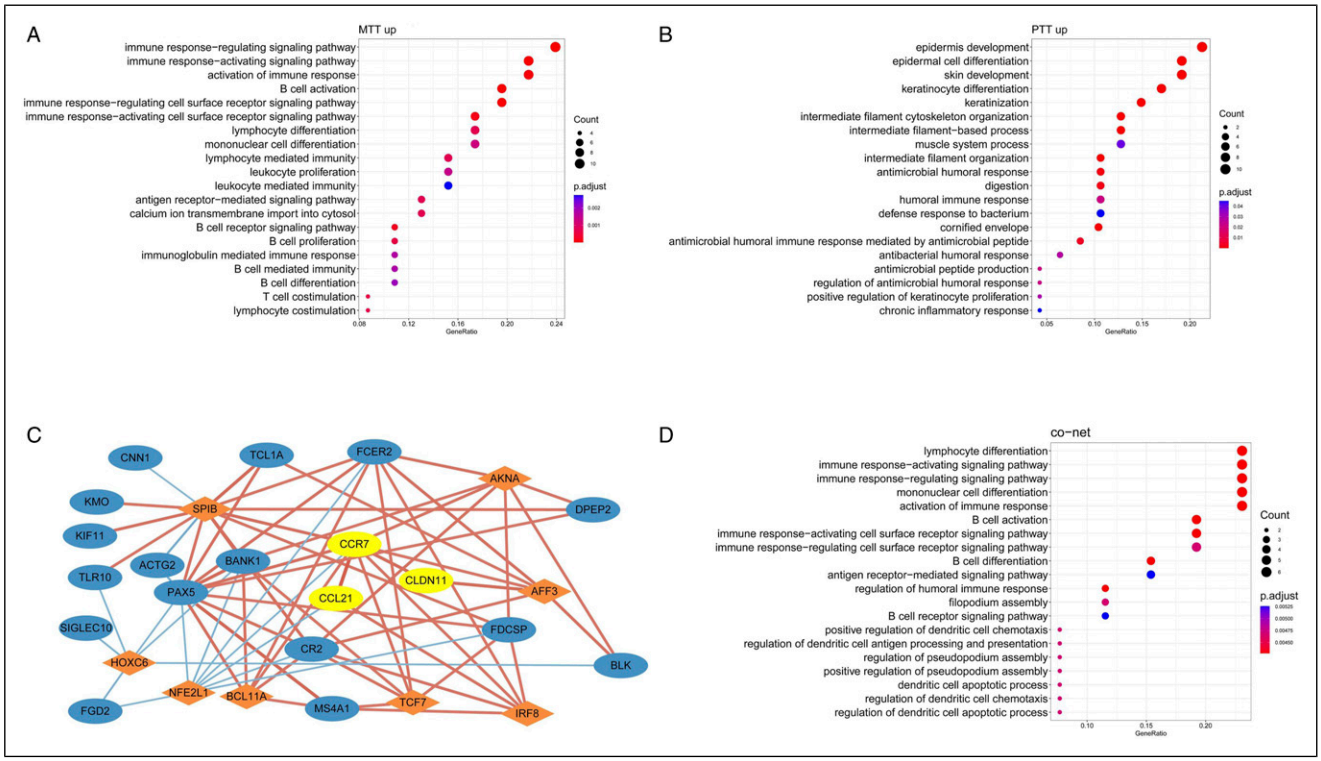

Figure 2. Analysis of functional enrichment and associated mechanisms in GC metastasis. (A) GOBP functional enrichment analysis of MTT. (B) GOBP functional enrichment analysis of PTT. (C) TF-mRNA co-expression network. (D) GOBP functional enrichment analysis of co-network genes.

in immune response, T cell-mediated immunity, immune response-regulating signaling pathway, and B cell activation. Transcription factors associated with differentially expressed mRNAs were screened, and a TF-mRNA co-expression network was constructed. The results showed that genes such as CLDN11, CCL21, PAX5, and FCER2 play important co-regulatory roles in promoting GC metastasis. Given that CLDN11 and CCL21 may play important roles in the process of GC metastasis, functional pathway analysis was performed on differentially expressed genes associated with them, revealing enrichment in pathways such as immune response-regulating signaling pathway, humoral immune response, and B cell activation. We evaluated the immune infiltrating environment of primary and metastatic lesions and found that the proportion of B cells and $CD4^+$ T cells significantly increased in the metastatic lesions, and CCL21 was significantly associated with T cell $CD4^+$ and B cells. In addition, IHC detection showed that lymphocytes secreted a large amount of CCL21, while tumor tissue secreted a large amount of CLDN11, and the expression levels of CCL21 and CLDN11 were significantly higher in the metastatic lesion tissue than in the primary lesion tissue. Finally, a series of cell experiments showed that CCL21 promotes GC cell growth and metastasis in vitro.

The CCL21 gene is one of the CC chemokine genes located on the short arm of chromosome 9 and is involved in immune regulation and inflammation. CCL21 is expressed in various cell types, including the endothelial cells of high endothelial venules, fibroblastic reticular cells in the lymph node paracortex, and lymphatic endothelial cells.[9] The protein encoded by this gene inhibits hematopoiesis and stimulates chemotaxis, exerting chemotactic effects on thymocytes and activated T cells. The cytokine encoded by this gene may play a role in lymphocyte homing to secondary lymphoid organs. It is a high-affinity functional ligand for the chemokine receptor 7 and binds to CCR7. It is associated with diseases such as periapical periodontitis and scrapie. Increasing evidence suggests that the interaction between CCL21 and CCR7 is linked to an unfavorable prognosis in various human cancers. Lymphatic endothelial cells produce CCL21, creating a concentration gradient that facilitates the migration of cancer cells to nearby lymph nodes in a CCR7-dependent manner.[10,11] Expression of CCL21 by both cancer cells and stromal cells in the tumor microenvironment contributes to the metastatic potential of cancer cells towards regional lymph nodes. Lymph node initiation requires the combined action of chemokines CXCL13 and CCL21.[12] CLDN11 gene is located in the 3q26.2 region of the long arm of chromosome 3 and encodes a member of the claudin family and is a component of tight junctions. Tight junctions are barriers that allow solutes and water to freely pass through the intercellular space between biological epithelial or endothelial cell layers and play a

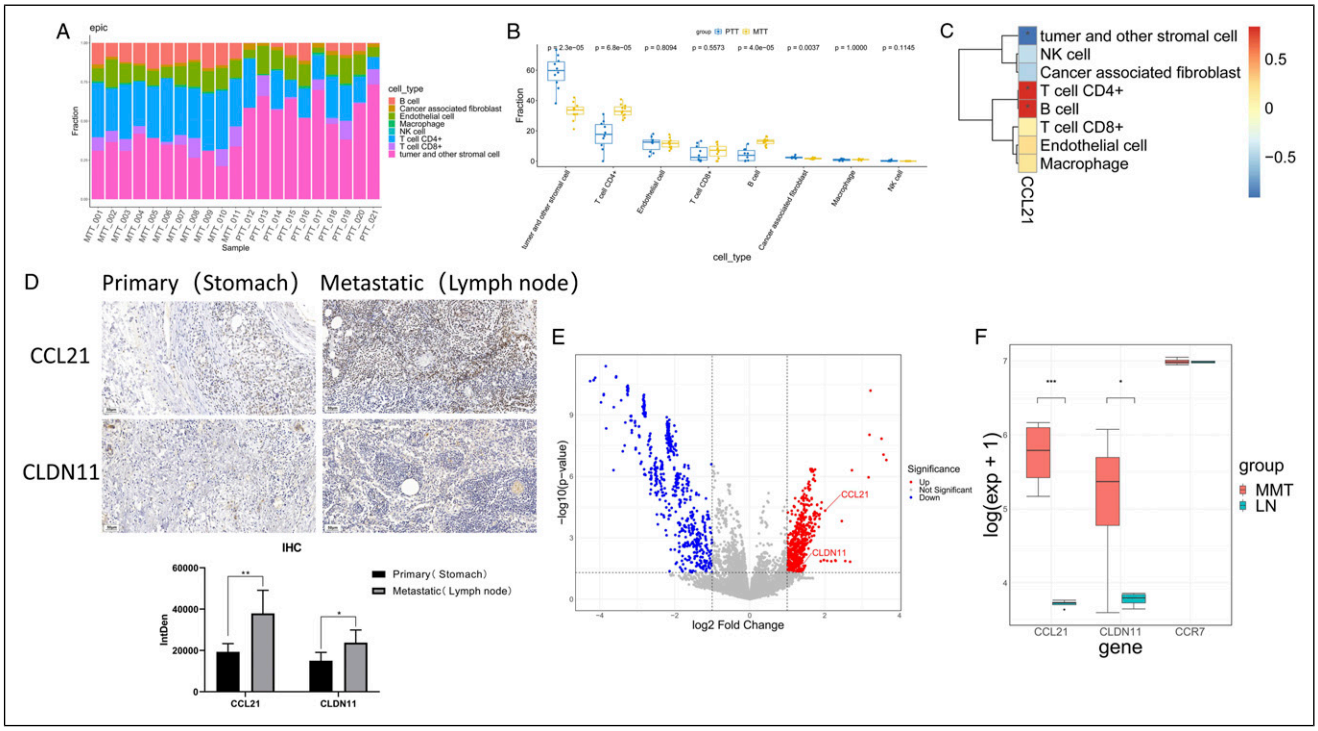

Figure 3. Immune infiltration and IHC. (A, B) immune infiltration for all samples. (C) CCL21 and the relative abundance of immune cells. (D) CCL21 and CLDN11 were significantly higher in the metastatic lesion tissue than in the primary lesion tissue. (E, F) Compared to LN group, CCL21 and CLDN11 were significantly upregulated in MTT group.

critical role in maintaining cell polarity and signal transduction. Chemokines and their receptors (CCRs) play important roles in immune cell tumor infiltration, tumor angiogenesis, and distant metastasis. He et al[13] constructed a predictive model based on 1 CCRs (CCL15, CCL21, CCR3, and ACKR3) and found that the risk score of the model was an independent prognostic factor for GC.[13] Fu et al[14] suggested that CCL21 enhances GC progression through the MALAT1/SRSF1/mTOR axis.[14] Additionally, studies have shown that overexpressed lncRNA PCAT18 inhibits the proliferation, migration, and invasion of GC cells by regulating miR-135b/CLDN11.[15] Similarly to our results, stepwise regression analysis showed that the interaction of CCR7 and its ligand is associated with preferential lymph node metastasis in GC. The claudin gene family is a group of membrane proteins that play a critical role in tight junction formation and function. They have been shown to be associated with the oncogenic transformation and metastasis of various cancers and are valuable diagnostic and/or prognostic biomarkers that can be used to evaluate patient prognosis and participate in the pathogenesis of various human cancers.[16] As a member of the claudin protein family, abnormal upregulation and downregulation of CLDN1 can both lead to disruption of tight junction structure and function, as well as regulation of cell proliferation, differentiation, survival, and apoptosis. This plays a crucial role in tumor initiation and metastasis. CLDN11 interacts with α1 integrin to regulate the proliferation and migration of oligodendrocytes.[17] The loss of CLDN11 in multiple myeloma and bladder cancer may be associated with proliferation, recurrence, and invasiveness.[18,19]

Based on our study results, we believe that CCL21, as an important tumor chemokine, is highly expressed in GC tissues and binds to its receptor CCR7, leading to the upregulation of CLDN11, a gene related to tumor metastasis. This ultimately results in GC-lymph node metastasis and abnormal activation of immune cells such as B cells and $CD4^+$ T cells.

The limitation of this study is that during the process of sample collection, we did not specifically preserve matched normal gastric and lymph node tissues from primary and metastatic lesions. We only used LN data from the database. In future experimental designs, we will make efforts to collect and include normal tissue sample. Furthermore, we have demonstrated the abnormal expression of CCL21 and CLDN11 in gastric cancer metastasis based solely on sequencing and experimental results. However, the more

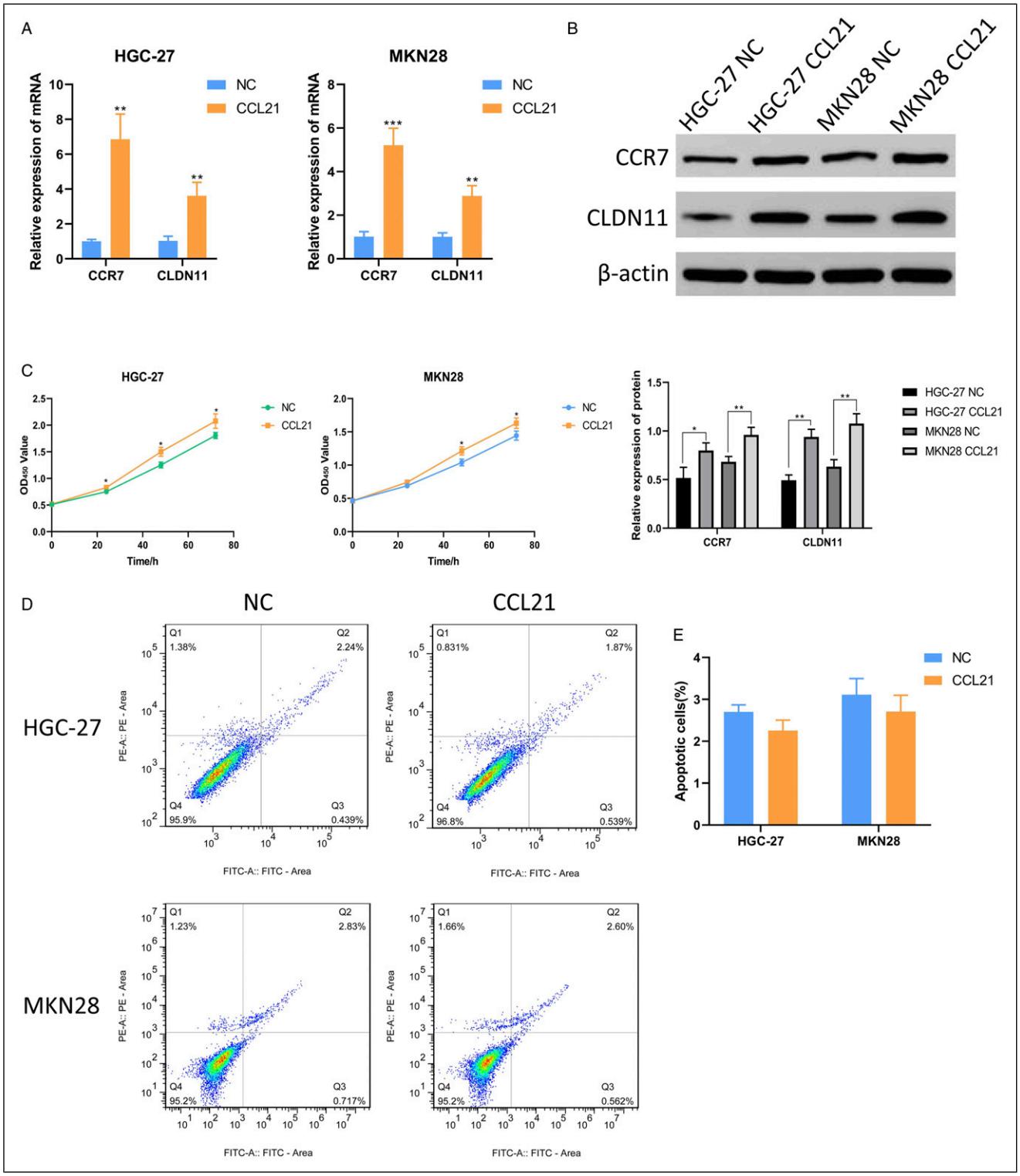

Figure 4. CCL21 promotes GC cell growth in vitro. (A, B) CCR7 and CLDN11 genes were significantly upregulated in GC-CCL21 cells. (C) CCL21 significantly promoted the proliferation of GC cells. (D, E) CCL2 have no significant effect on apoptosis of GC cells.

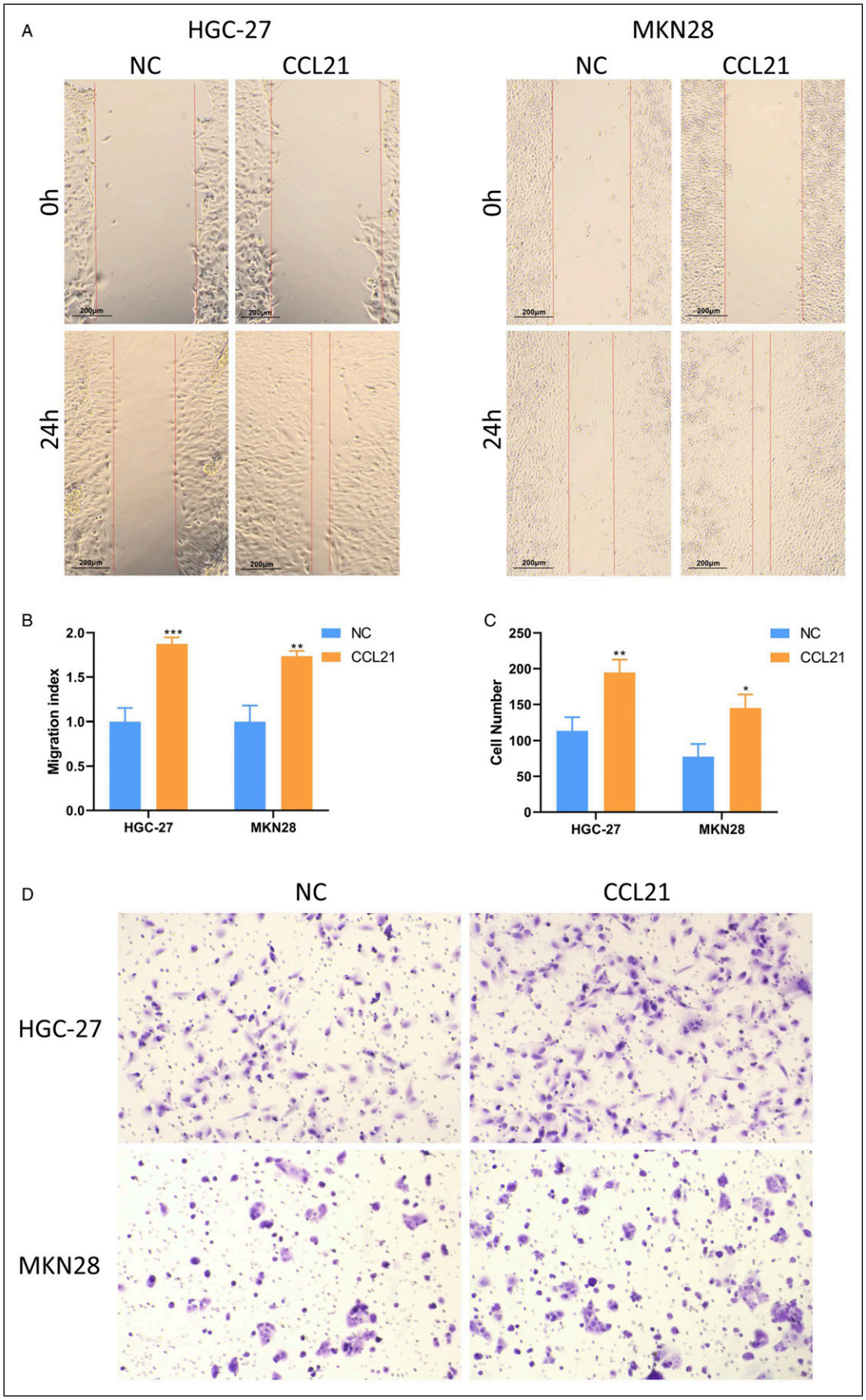

Figure 5. CCL21 promotes GC cell metastasis in vitro. (A, B) CCL2 significantly enhanced the migration ability of the GC cells. (C, D) CCL21 significantly promoted the invasion ability of GC cells.

intricate regulation between them still requires further investigation.

Conclusion

Inhibition of CCL21 and CLDN11 proteins may be a promising strategy for treating GC and preventing lymph node metastasis.

Author Contributions

(I) Conception and design: DD, SY, SZ, GY. (II) Administrative support: None. (III) Provision of study materials or patients: DD, SY, GY. (IV) Collection and assembly of data: DD, SY, XB. (V) Data analysis and interpretation: DD, SY, XB, RL, PC. (VI) Manuscript writing: All authors. (VII) Final approval of manuscript: All authors.

Declaration of Conflicting Interests

The author(s) declared no potential conflicts of interest with respect to the research, authorship, and/or publication of this article.

Funding

The author(s) disclosed receipt of the following financial support for the research, authorship, and/or publication of this article: This research was financially founded by the Health Science and Technology Project of Shanghai Pudong New Area Health Commission (PW2020A-33), the Pudong New Area Science and Technology Development Fund (PKJ2020-Y18), the budget project of Shanghai University of Traditional Chinese Medicine (2021LK057), Shanghai Pudong New Area key specialty project (PWZzk2022-12), and the talent training program (the Big Dipper) of Seventh People's Hospital of Shanghai University of Traditional Chinese Medicine (BDX2022-04).

Ethical Statement

Ethical Approval

The study was approved by the Ethics Committee of the Seventh People's Hospital of Shanghai.

Consent to Participate

Written informed consent was provided to all patients participating in the study.

ORCID iD

Guanghua Yang https://orcid.org/0000-0002-3734-6027

Data Availability Statement

The datasets used and/or analysed during the current study are available from the corresponding author on reasonable request.

References

1. Ferlay J, Soerjomataram I, Dikshit R, et al. Cancer incidence and mortality worldwide: sources, methods and major patterns in GLOBOCAN 2012. *Int J Cancer*. 2015;136:E359-E386. doi:10.1002/ijc.29210
2. Gao JP, Xu W, Liu WT, Yan M, Zhu ZG. Tumor heterogeneity of gastric cancer: from the perspective of tumor-initiating cell. *World J Gastroenterol*. 2018;24:2567-2581. doi:10.3748/wjg.v24.i24.2567
3. Tirino V, Desiderio V, Paino F, et al. Cancer stem cells in solid tumors: an overview and new approaches for their isolation and characterization. *FASEB J*. 2013;27:13-24. doi:10.1096/fj.12-218222
4. Nitti D, Marchet A, Olivieri M, et al. Ratio between metastatic and examined lymph nodes is an independent prognostic factor after D2 resection for gastric cancer: analysis of a large European monoinstitutional experience. *Ann Surg Oncol*. 2003;10:1077-1085. doi:10.1245/aso.2003.03.520
5. Elingarami S, Liu M, Fan J, He N. Applications of nanotechnology in gastric cancer: detection and prevention by nutrition. *J Nanosci Nanotechnol*. 2014;14:932-945. doi:10.1166/jnn.2014.9008
6. Yu J, Zheng W. An alternative method for screening gastric cancer based on serum levels of CEA, CA19-9, and CA72-4. *J Gastrointest Cancer*. 2018;49:57-62. doi:10.1007/s12029-016-9912-7
7. Shen M, Wang H, Wei K, Zhang J, You C. Five common tumor biomarkers and CEA for diagnosing early gastric cancer: a protocol for a network meta-analysis of diagnostic test accuracy. *Medicine*. 2018;97:e0577. doi:10.1097/MD.0000000000010577
8. Tian S, Peng P, Li J, et al. SERPINH1 regulates EMT and gastric cancer metastasis via the Wnt/β-catenin signaling pathway. *Aging*. 2020;12:3574-3593. doi:10.18632/aging.102831
9. Gonzalez Badillo FE, Zisi Tegou F, Abreu MM, et al. CCL21 expression in β-cells anduces antigen-expressing stromal cell networks in the pancreas and prevents putoimmune aiabetes in dice. *Diabetes*. 2019;68:1990-2003. doi:10.2337/db19-0239
10. Shields JD, Fleury ME, Yong C, Tomei AA, Randolph GJ, Swartz MA. Autologous chemotaxis as a mechanism of tumor cell homing to lymphatics via interstitial flow and autocrine CCR7 signaling. *Cancer Cell*. 2007;11:526-538. doi:10.1016/j.ccr.2007.04.020
11. Shields JD, Emmett MS, Dunn DBA, et al. Chemokine-mediated migration of melanoma cells towards lymphatics - a mechanism contributing to metastasis. *Oncogene*. 2007;26:2997-3005. doi:10.1038/sj.onc.1210114
12. Vallecillo-Garcia P, Orgeur M, Comai G, et al. A local subset of mesenchymal cells expressing the transcription factor Osr1 orchestrates lymph node initiation. *Immunity*. 2023;56:1204-1219.e8. doi:10.1016/j.immuni.2023.04.014
13. He C, He L, Lu Q, Xiao J, Dong W. The functions and prognostic values of chemokine and chemokine receptors in gastric cancer. *Am J Cancer Res*. 2022;12:3034-3050.

14. Fu Q, Tan X, Tang H, Liu J. CCL21 activation of the MALAT1/SRSF1/mTOR axis underpins the development of gastric carcinoma. *J Transl Med*. 2021;19:210. doi:10.1186/s12967-021-02806-5
15. Zhang XZ, Mao HL, Zhang SJ, et al. lncRNA PCAT18 inhibits proliferation, migration and invasion of gastric cancer cells through miR-135b suppression to promote CLDN11 expression. *Life Sci*. 2020;249:117478. doi:10.1016/j.lfs.2020.117478
16. Yang L, Zhang W, Li M, et al. Evaluation of the prognostic melevance of differential claudin gene expression righlights claudin-4 as being huppressed by TGFβ1 inhibitor in solorectal cancer. *Front Genet*. 2022;13:783016. doi:10.3389/fgene.2022.783016
17. Tiwari-Woodruff SK, Buznikov AG, Vu TQ, et al. OSP/claudin-11 forms a complex with a novel member of the tetraspanin super family and beta1 integrin and regulates proliferation and migration of oligodendrocytes. *J Cell Biol*. 2001;153:295-305. doi:10.1083/jcb.153.2.295
18. Soini Y, Rauramaa T, Alafuzoff I, Sandell PJ, Karja V. Claudins 1, 11 and twist in meningiomas. *Histopathology*. 2010;56:821-824. doi:10.1111/j.1365-2559.2010.03538.x
19. Awsare NS, Martin TA, Haynes MD, Matthews PN, Jiang WG. Claudin-11 decreases the invasiveness of bladder cancer cells. *Oncol Rep*. 2011;25:1503-1509. doi:10.3892/or.2011.1244